ELSEVIER

Journal of Structural Geology 28 (2006) 1208–1213

JOURNAL OF STRUCTURAL GEOLOGY

www.elsevier.com/locate/jsg

# The moment method used to infer stress from fault/slip data in sigma space: invalidity and modification

Yehua Shan [a,*], Norman Fry [b]

[a] *Computational Geosciences Research Center, Central South University, Changsha City 410083, P.R. China*
[b] *School of Earth, Ocean and Planetary Sciences, Cardiff University, Cardiff CF10 3YE, UK*

Received 12 September 2005; received in revised form 24 February 2006; accepted 3 March 2006
Available online 8 May 2006

**Abstract**

The moment method has recently been used to infer stress in sigma space from fault/slip data. However, if these data are distributed along a hyperplane having a smaller dimension than that of the space minus one, due to limited fault/slip population or biased sampling of it, the best solution of stress vector is not in most cases, as expected, the eigenvector of the datum matrix relating to the smallest eigenvalue. The solution lies within the subspace composed of the eigenvectors relating to the small eigenvalues, for which some auxiliary constraints need to be included. Shear sense constraint alone is adopted, and incorporated by way of grid search, which gives rise to a range of accepted stress vectors in the subspace. Examples from the Chelungpu fault, Taiwan, illustrate the feasibility of the proposed scheme.


*Keywords:* Stress inversion; Sigma space; Fault/slip data; Moment method; Biased sampling; Indeterminacy

## 1. Introduction

Although stress inversion appears nonlinear in character, Fry (1999) transformed fault/slip data into datum vectors in 'sigma space' where they tend to be distributed in or near a hyperplane if they were produced in a single tectonic phase. In contrast to some conventional nonlinear schemes (e.g. Angelier, 1984; Xu, 2004), this justifies a new, for the most part linear, scheme for inversion of stress. For single-phase (or homogeneous) data, there is an analytical solution for the 'stress vector' directed normal to the hyperplane. It is the eigenvector corresponding to the fifth largest eigenvalue of the data matrix. (This is the smallest in the 5D space of Shan et al. (2003), but the second smallest of Fry (1999) because he retained the irresolvable (isotropic stress) sigma axis.) This is known as the moment method, as the eigenvector is that of the second moment (or Scheidegger) tensor, composed of second moments—the moments and products of inertia—of the data set. Eigenvector polarity is not constrained in the determination. So, for any solution, its negative is equally valid. Completion of the stress inversion, by discriminating between polarities, requires knowledge of observed fault slip senses, which are not taken into account within the moment method.

It is generally implicit in this scheme that the estimated stress vector should be the unique parameter that best describes the planar distribution of datum vectors in sigma space. Uniqueness requires full dimensionality of the hyperplane of datum vectors of the four dimensions, after conventional 'reduction' to remove indeterminacies (Fry, 1999). Lower dimensionality increases the degrees of freedom of the solution (Fry, 1999).

While recently applying the scheme to real data sets of probably a single phase, we found that this implicit condition is often not fulfilled. Some of them will be discussed below. In these real cases, the hyperplane has smaller dimensionality. So, the stress vector associated with the smallest eigenvector, rather than being a unique solution, is one member of a range of solutions represented by a plane or volume in sigma space. Fry (1999) introduced an unrelated geometric space—'q-space'—in which the distribution of the data through this range could be considered in combination with known shear senses. The aim of this communication is to develop a practical alternative modification, in which treatment of shear sense is integrated into sigma space, rather than subsequent to it.

* Corresponding author. Tel.: +86 20 85290763; fax: +86 20 85290130
*E-mail address:* shanyehua@yahoo.com.cn (Y. Shan).

0191-8141/$ - see front matter © 2006 Elsevier Ltd. All rights reserved.
doi:10.1016/j.jsg.2006.03.002

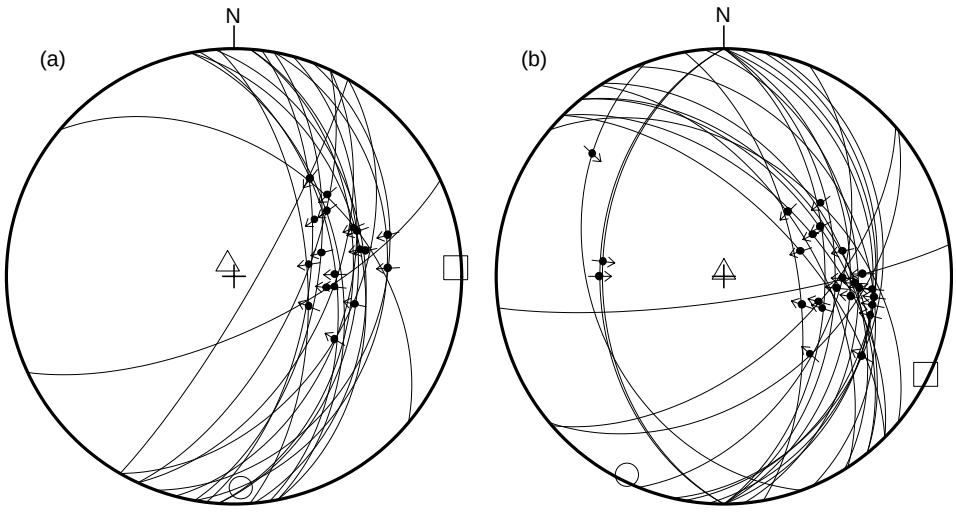


Fig. 1. Equal-area, lower hemispheric projection of fault/slip data measured at segments D (a) and C (b) of the Chelungpu fault, respectively. Fault data (Lee et al., 2002) were provided by Blenkinsop (in press). Unfilled squares, circles and triangles represent the maximum, the intermediate and the minimum principal axes, respectively. They represent the stress tensor restored from the geometric mean values of accepted stress vectors.

## 2. An example showing the failure of the simple moment method

To show the phenomenon described above, an example is taken from Lee et al. (2003), as modified by Blenkinsop (2006). It consists of 18 fault/slip data (Fig. 1a) from segment D of the active Chelungpu fault, western Taiwan. (See Blenkinsop (in press) for descriptive summary, context and comparative analyses.) These surface rupture data had been produced during the 1999 Chi-Chi earthquake along the Chelungpu fault (Lee et al., 2002, 2003; Angelier et al., 2003). All slip senses were reverse and generally plunging towards the east (Fig. 1). Application of the moment method (Fry, 1999; Shan et al., 2004) to the data set gives rise to results listed in Tables 1 and 2.

In Table 1, all the eigenvectors of the datum matrix are listed in descending order of eigenvalue. The eigenvector relating to the smallest eigenvalue, symbolised as $\boldsymbol{v}_5$, represents the best solution of stress vector. However, neither the positive vector nor its negative ($-\boldsymbol{v}_5$) accords with all observed slip senses (Table 2); only 38 and 61% satisfy the real senses of the fault data, respectively. Of their corresponding stress tensors, the maximum principal direction is 175.93° in the former and 76.07° in the latter. They are approximately perpendicular to each other. The possibility of two such diverse phases in the data set is not supported by the fact that these data were produced along a single reactivation of the fault during the 1999 Chi-Chi earthquake (Lee et al., 2002). Meanwhile, although measurement errors surely exist, it is very difficult or even impossible for them, in the light of their stochastic nature, to produce the two phases having nearly perpendicular maximum principal directions.

## 3. Reason for the failure

In seeking a unique solution by the moment method, it is implicitly assumed that the eigenvector of the data matrix relating to the smallest eigenvalue is a unique parameter that describes the hyperplane. This assumption does not hold in cases that, when eigenvalues are taken in decreasing order, give an abrupt reduction to low eigenvalue after less than four of them. In such a case, the hyperplane of data is effectively reduced in dimensions from 4 to 3, 2 or even 1. A mundane reason for such a reduction can be biased sampling of fault data at outcrop. For example, repetitious sampling of a single fault set would make fault data vectors cluster in sigma space, probably reducing the dimension of the hyperplane to 1. A more serious concern is that such a reduction can be an inherent

Table 1
Eigenvalues and corresponding eigenvectors ($\boldsymbol{v}_i$, $i=1, 2,\ldots,5$) of the data matrix for the example from segment D of the Chelungpu fault. The last row is the geometric mean vector ($\boldsymbol{v}$) according to the method in this paper, being a compromise linear combination of three selected eigenvectors with coefficients as, $\boldsymbol{v}=0.146\boldsymbol{v}_5+0.899\boldsymbol{v}_4+0.412\boldsymbol{v}_3$. See the text for more explanation

| No. | Eigenvalues | Eigenvectors | | | | | |
|---|---|---|---|---|---|---|---|
| | | Symbols | $\sigma_{11}$ | $\sigma_{22}$ | $\sigma_{12}$ | $\sigma_{13}$ | $\sigma_{23}$ |
| 1 | 12.8616 | $\boldsymbol{v}_1$ | 0.093 | 0.159 | −0.696 | 0.068 | 0.691 |
| 2 | 3.6694 | $\boldsymbol{v}_2$ | −0.221 | 0.638 | −0.097 | 0.676 | −0.281 |
| 3 | 0.8632 | $\boldsymbol{v}_3$ | 0.388 | 0.471 | 0.631 | −0.029 | 0.478 |
| 4 | 0.5538 | $\boldsymbol{v}_4$ | 0.864 | 0.080 | −0.277 | −0.004 | −0.414 |
| 5 | 0.0516 | $\boldsymbol{v}_5$ | 0.215 | −0.583 | 0.177 | 0.733 | 0.211 |
| 6 | | $\boldsymbol{v}$ | 0.968 | 0.181 | 0.037 | 0.091 | −0.144 |

Table 2
For the example from segment D of the Chelungpu fault, principal stress directions and stress ratios for the eigenvectors relating to the three smallest eigenvalues and for the geometric mean stress vectors. For comparison, Celerier's (personal communication, 2005) result by running his FAS software (Celerier, 1999) was also listed in the second last row. For comparison, stress inversion from focal mechanisms in the region by Kao and Angelier (2001) is also shown at the last row. Fit percentage is the percent of the observed slip senses similar to the calculated ones under the estimated stress. Stress ratio is defined as $(\sigma_2-\sigma_3)/(\sigma_1-\sigma_3)$, where $\sigma_1$, $\sigma_2$ and $\sigma_3$ are the maximum, the intermediate and the minimum principal stresses, respectively. Compressional stress is positive while tensional stress is negative.

| No. | Vectors | Fit percentage (%) | Principal directions (°) | | | | | | Stress ratio |
|---|---|---|---|---|---|---|---|---|---|
| | | | $\sigma_1$ | | $\sigma_2$ | | $\sigma_3$ | | |
| | | | Bearing | Plunge | Bearing | Plunge | Bearing | Plunge | |
| 3 | $\boldsymbol{v}_3$ | 88 | 40.50 | 9.88 | 306.61 | 21.26 | 153.93 | 66.35 | 0.55 |
| | $-\boldsymbol{v}_3$ | 12 | 153.93 | 66.35 | 306.61 | 21.26 | 40.50 | 9.88 | 0.45 |
| 4 | $\boldsymbol{v}_4$ | 100 | 109.26 | 3.98 | 200.70 | 19.82 | 8.39 | 69.75 | 0.40 |
| 5 | $\boldsymbol{v}_5$ | 38 | 175.93 | 9.02 | 273.97 | 41.40 | 76.07 | 47.18 | 0.11 |
| | $-\boldsymbol{v}_5$ | 61 | 76.07 | 47.18 | 273.97 | 41.40 | 175.93 | 9.02 | 0.89 |
| 6 | $\boldsymbol{v}$ | 100 | 87.77 | 2.31 | 178.03 | 6.26 | 337.64 | 83.32 | 0.36 |
| 7 | Celerier's result | | 97.25 | 12.84 | 189.71 | 10.68 | 318.31 | 73.18 | 0.62 |
| 8 | Kao and Angelier's (2001) result | | 295 | 4 | 28 | 35 | 199 | 54 | 0.29 |

aspect of the fault population being sampled. In the case of reactivated faults, there may be insufficient range of pre-existing fault orientations. Or the orientations that reactivate may be severely restricted by frictional limitations on slip. The limiting case to such restrictions corresponds to that of previously unfractured rock, for which a poorly 2D hyperplane (plane) contains the two clusters from conjugate fault sets. Away from these severely limited cases, the dimensional extent of a data set in sigma space cannot generally be judged from the raw data or from stereographic representations of their real space orientations.

For the given example, we look at the eigenvalues of the data matrix (Table 1), as they reflect the distribution of datum vectors in sigma space. With respect to the two largest eigenvalues, 12.8616 and 3.6694, the three other eigenvalues, 0.8632, 0.5538 and 0.0516, are very small. This indicates that the datum vectors have a strong tendency of being distributed close to a 2D plane, within which there is also a tendency to alignment along the eigenvector relating to the largest eigenvalue. The lack of constraint on stress by these data, manifested in loss of hyperplane dimensionality, is sufficiently stark as to be evident as lack of variation in orientations in real space (Fig. 1a). The hyperplane, towards which datum vectors are distributed, is reduced from 4 to 2 dimensions. Consequently, the reduced hyperplane leaves two residual degrees of freedom for the stress solution. This lies within the range represented geometrically in sigma space by the residual volume corresponding to combinations of the eigenvectors relating to the first, the second and the third smallest eigenvalues.

Furthermore, within the residual volume, in this circumstance, small fluctuations inherent in empirical data, due to measurement errors or slight departure from the assumption of constant stress state for the whole data set, may lead to a large discrepancy between the optimum stress vector and the eigenvector relating to the smallest eigenvalue. Therefore, in such cases of an ill-defined best stress vector, it is not improbable that the stress tensor constructed from the eigenvector relating to the smallest eigenvalue will be meaningless. Shear sense then becomes an indispensable element of the stress determination.

## 4. Modification of the moment method

As stated above, a number greater than one, $k$ let us say, of eigenvectors having small value, is needed to describe the range of normals to the hyperplane of datum vectors in the sigma space. By definition, the best solution ($\boldsymbol{v}$) of stress vector lies in the subspace defined by these eigenvectors ($\boldsymbol{v_i}$, $i=5-k+1,\ 5-k+2,\ldots,5$) of the sigma space and is a linear combination of them:

$$v = \sum_{i=5-k+1}^{5} a_i v_i \tag{1}$$

where $a_i$ are the unknown coefficients. Only in the simple case of $k=1$ does $a_i=1$ and $\boldsymbol{v}=\boldsymbol{v}_5$, otherwise, $a_i$ are unknown.

In order to solve for these unknown coefficients some auxiliary constraint(s) must be included. A minimum condition to be incorporated is that a single phase should account for all, or at least as many as possible, observed slip senses. This is complicated by virtue of the nonlinear character of the constraint. For the sake of simplicity, we use in this paper a grid-searching method that discretises the subspace into a series of densely spaced nodes and accepts as stress vector the node best satisfying the constraint.

The method is simple in theory and easy to program, compared with sophisticated optimization algorithms that may be used for the task but are beyond the scope of this paper.

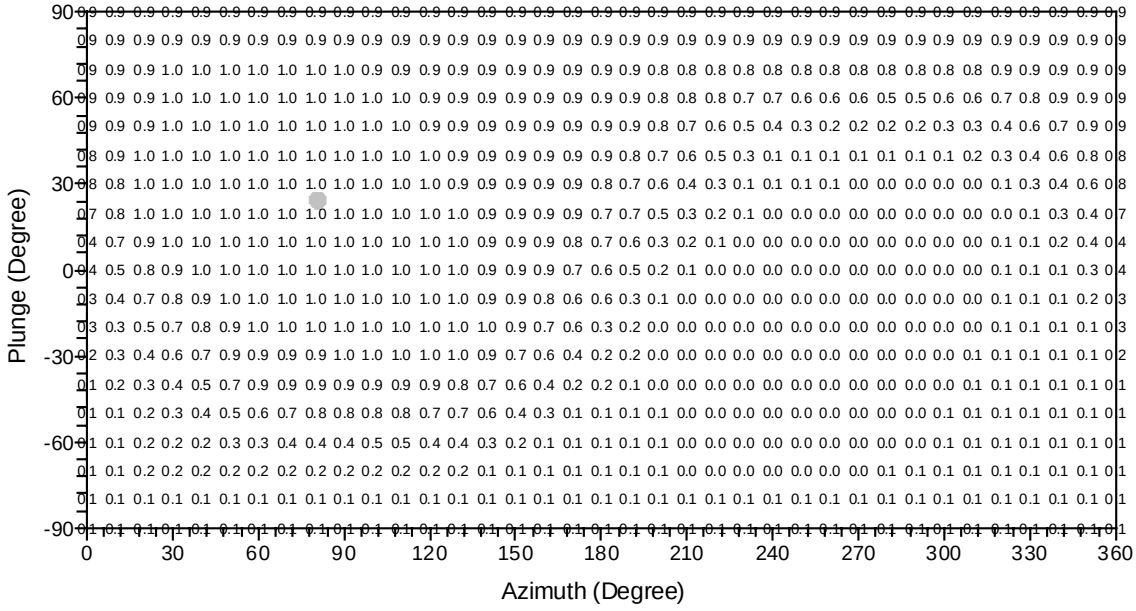


Fig. 2. The distribution of the proportion of data at segment D that fit the node conditions, in evenly 10° spaced azimuths and plunges. The grey dot in the left side, with an azimuth of 80.8° and a plunge of 24.3°, represents the solution of geometric mean stress vector when using the constraint. See the text for definitions of the azimuth and plunge and explanation.

Also beyond the scope of this paper are additional constraints such as friction.

## 5. Test

Two examples are taken to show the feasibility of the grid search proposed above. They have 2D and 3D reduced hyperplanes, respectively, toward which datum vectors are distributed in the sigma space.

### *5.1. Example with a 2D reduced hyperplane*

For the above example, we take the 3D section through sigma space containing the eigenvectors relating to the three smallest eigenvalues (Table 1). We represent this subspace with $\boldsymbol{v}_5$, $\boldsymbol{v}_4$ and $\boldsymbol{v}_3$ directed eastwards, northwards and upwards, respectively, and consider directions from the centre as intersection points on a unit sphere centred at the origin. For grid definition, we describe any point on the sphere by its azimuth and plunge. The azimuth starts from the eastern direction and increases anticlockwise. The ranges of the azimuth (from 0 to 360°) and of the plunge (from −90 to 90°) are each evenly spaced every 10°. A smaller spacing would lead to a higher precision of stress vector, but takes a longer time. Note that this is not an equal density mesh; as grid points are closer at high absolute values of plunge, the azimuthal resolution will be greater the higher the absolute plunge. However, this does not invalidate the method and the prescribed spacing is sufficient to illustrate our example, the results of which are shown in Figs. 1–3, and listed in Tables 1 and 2.

In the central left side of Fig. 2, the fit proportion reaches 1.0 within an approximately elliptical range. This means that all observed slip senses are consistent with a solution of stress vector, provided it lies in this range. Without further constraints, we cannot theoretically exclude any stress vector within the range. It should, nevertheless, be noted that nodes at the margin of this field will have at least one datum for which the resolved shear stress is close to switching sense, which implies that it is minimal in value and that slip on the fault concerned would be highly unlikely to occur. So, the true stress solution is likely to be represented well inside this field, not by a node at its margin.

Fig. 3a shows stress tensors that were converted from these accepted vectors. Both the maximum and the minimum principal directions are restricted to patches around E–W and upwards, respectively. The former has a wider distribution than the latter, indicating tighter constraint on the latter. Meanwhile, the intermediate principal directions are restricted to an incomplete great circle.

As an example of a selection of a unique stress state from within this range, a geometric mean vector (Table 1 and Fig. 1a) has been calculated from all the accepted stress vectors in the range. (There is no theoretical preference for geometric mean. If there were, it would become important to use an evenly spaced grid. We simply choose the same well-known, transparent and identical specification, for each example in this paper, for achieving a reasonably representative central value.) Its converted stress tensor (Fig. 1 and Table 2) has a maximum principal stress of azimuth 87.77°. The direction is quite well in accordance with the assumed regional E–W compression (Kao and Angelier, 2001) (Table 2) and also is similar to that

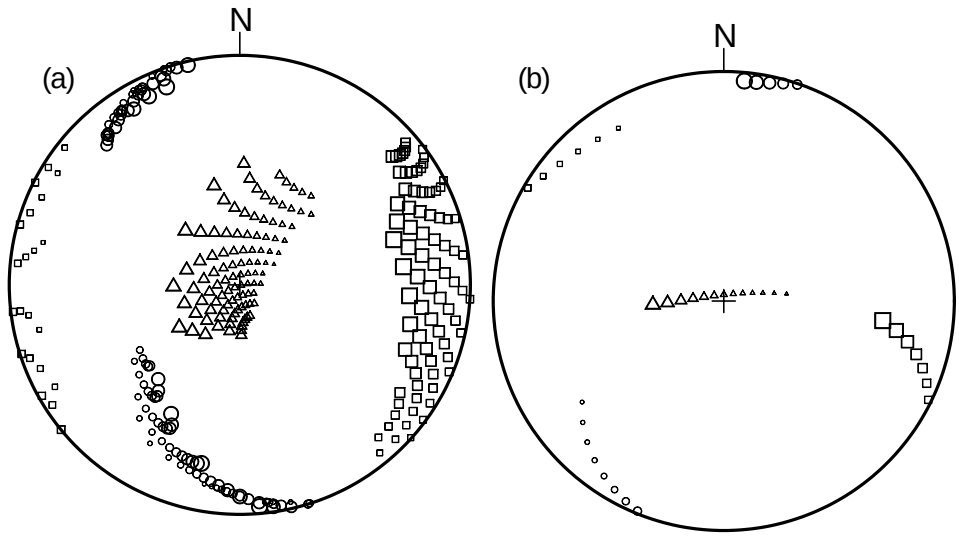


Fig. 3. Equal-area, lower hemispheric projection of accepted stress tensors inferred from fault/slip data from segments D (a) and C (b) of the Chelungpu fault, respectively. Unfilled squares, circles and triangles represent the maximum, the intermediate and the minimum principal axes, respectively. Stress ratio is characterised by the symbol size, ranging from 0.064 to 0.868 in (a) and from 0.193 to 0.829 in (b). See the caption of Table 2 for its definition.

Table 3
Eigenvalues and corresponding eigenvectors ($\boldsymbol{v}_i$, $i=1, 2,\ldots,5$) of the data matrix for the example from segment C of the Chelungpu fault. In the last row, the geometric mean stress vector ($\boldsymbol{v}$) is a compromise linear combination of two selected eigenvectors with coefficients as $\boldsymbol{v}=0.1740\boldsymbol{v}_5+0.985\boldsymbol{v}_4$

| No | Eigenvalues | Eigenvectors | | | | | |
|---|---|---|---|---|---|---|---|
| | | Symbols | $\sigma_{11}$ | $\sigma_{22}$ | $\sigma_{12}$ | $\sigma_{13}$ | $\sigma_{23}$ |
| 1 | 14.0142 | $\boldsymbol{v}_1$ | −0.014 | −0.279 | −0.521 | −0.154 | 0.792 |
| 2 | 5.8789 | $\boldsymbol{v}_2$ | −0.283 | 0.666 | −0.095 | 0.621 | 0.288 |
| 3 | 3.1538 | $\boldsymbol{v}_3$ | 0.320 | 0.073 | 0.778 | −0.060 | 0.532 |
| 4 | 0.8743 | $\boldsymbol{v}_4$ | 0.820 | 0.441 | −0.337 | −0.117 | −0.074 |
| 5 | 0.0787 | $\boldsymbol{v}_5$ | 0.381 | −0.528 | −0.018 | 0.757 | −0.044 |
| 6 | | $\boldsymbol{v}$ | 0.874 | 0.343 | −0.335 | 0.017 | 0.081 |

calculated by alternative algorithms, e.g. by Celerier (personal communication, 2005) (Table 2).

### 5.2. Example with a 3D reduced hyperplane

This example is taken from segment C of the same Chelungpu fault. It consists of 24 fault/slip data, mainly distributed in two fault sets (Fig. 1b). In Table 3, there exist two small eigenvalues, the smallest of which fails to accord with all shear senses, in either polarity. Therefore, we make a 2D subspace containing the eigenvectors relating to them, where $\boldsymbol{v}_5$ and $\boldsymbol{v}_4$ are directed eastwards and northwards, respectively. The azimuth is defined in the same way as in the previous subsection. The range of the azimuth is also evenly spaced every 10°.

Figs. 3b and 4 and Table 4 show results through applying the grid-search method to this example. On the stereogram, principal directions converted from the accepted vectors are distributed along lines, in accord with the single remaining degree of freedom. It is interesting to note that the maximum and minimum principal stress axes seem to fall within the field of possible axes for segment D, described in the previous subsection. However, there is no overlap for the intermediate principal axis. This suggests similarity rather than homogeneity of deformation field in the area. The common, fully shared, feature is the closeness

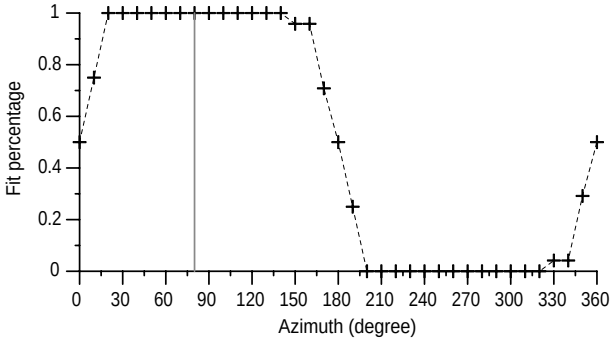


Fig. 4. The distribution of the proportion of data at segment C that fit the node conditions in 10° evenly spaced azimuths. The grey line in the left side, with an azimuth of 80°, represents the solution of geometric mean stress vector when using the constraint. See the text for more explanation.

Table 4
For the example from segment C of the Chelungpu fault, principal stress directions and stress ratios for the eigenvectors relating to the two smallest eigenvalues and for the geometric mean stress vector. See the caption of Table 2 for more explanation

| No. | Vectors | Fit percentage (%) | Principal directions (°) | | | | | | Stress ratio |
|---|---|---|---|---|---|---|---|---|---|
| | | | $\sigma_1$ | | $\sigma_2$ | | $\sigma_3$ | | |
| | | | Bearing | Plunge | Bearing | Plunge | Bearing | Plunge | |
| 4 | $v_4$ | 100 | 300.08 | 1.60 | 209.96 | 4.62 | 49.12 | 85.11 | 0.33 |
| 5 | $v_5$ | 50 | 341.46 | 22.29 | 230.52 | 41.09 | 92.06 | 40.64 | 0.03 |
| | $-v_5$ | 50 | 92.06 | 40.64 | 230.52 | 41.09 | 341.46 | 22.29 | 0.97 |
| 6 | $v$ | 100 | 115.91 | 1.28 | 205.97 | 2.67 | 0.28 | 87.04 | 0.38 |

of the minimum principal stress axis to the vertical (Tables 1 and 3).

## 6. Discussions and conclusions

As discussed above, the application of the moment method (Fry, 1999; Shan et al., 2003) to fault/slip data that offer poor constraint results in a reduced hyperplane in the sigma space and the eigenvector relating to the smallest eigenvalue need not give the best solution of stress vector. The linear combination of the eigenvectors relating to the small eigenvalues, to constrain a best stress solution, requires auxiliary constraints. The first choice is the empirical constraint, which match between observed and estimated slip senses. As shown in two examples from the Chelungpu fault, Taiwan, grid search in sigma space can still result in a range of accepted stress vectors. There may not be any reason to constrain this range further, to a unique solution. To do so requires either an arbitrary choice of a 'best' vector (e.g. geometric mean) or additional constraints extraneous to the data, such as a predetermined principal direction.

The lack of full dimensionality of the data hyperplane, highlighted in this paper, would present a severe problem for separating polyphase fault/slip data into single-phase subsets. Two single-phase data subsets would remain as a single unresolved set if there is overlap between the subspaces characterised by the eigenvectors relating to the small eigenvalues for each phase. It is important to realize that this problem is inherent in such data, regardless of the method used for stress inversion; it is not a weakness of the method. What the above discussion has done is to highlight this general problem in a manner that is amenable to geometrical appreciation, as was intended by Fry (1999). By any method, a good stress determination requires collection, not so much of a large number of data, but of data that, when considered as stress space vectors, spread as fully as possible through the dimensionality of sigma space (Fry, 1999).

Comparison of the use of subspaces of sigma space in this study and of 'q-space' from Fry (1999) shows that they are, in fact, the same. Both are defined by orthogonal axes, each of which represents a fractional contribution of the corresponding stress end member given by an eigenvector of the data. Whereas q-space was conceptualised (Fry, 1999) as being specified independently for each subset of data, the sigma space equivalent in this paper demonstrates that subspaces can be considered together, as having meaningful spatial relationships within the full sigma space of which each is a part.

## Acknowledgements

This work is funded by the Hundred Talent Program of Chinese Academy of Sciences (KZCX0543081001), and by the startup project of Computational Geosciences Research Center, Central South University. We are indebted to B. Celerier who pointed out the shortcoming of the moment method during reviewing another paper and provided his result of estimated stress using his software, and Tom Blenkinsop who provided the Chi-Chi data in a ready to use format. This paper was revised by M.D. Tranos and one anonymous referee who made valuable comments and suggestions of it.

## References

Angelier, J., 1984. Tectonic analysis of fault slip data sets. Journal Geophysical Research B89, 5835–5848.

Angelier, J., Lee, J.C., Hu, J.C., Chu, H.T., 2003. Three-dimensional deformation along the rupture trace of the September 21st, 1999, Taiwan earthquake: a case study in the Kuangfu school. Journal of Structural Geology 25, 351–370.

Blenkinsop, T.G., 2006. Kinematic and dynamic fault slip analyses: implications from the surface rupture of the 1999 Chi-Chi, Taiwan, earthquake. Journal of Structural Geology 28, 1040–1050.

Celerier, B., 1999. FSA.18: Fault Slip Analysis Software, http://www.isteem.univ-montp2.fr/PERSO/celerier/software/fsa18.html.

Fry, N., 1999. Striated faults: visual appreciation of their constraint on possible palaeostress tensors. Journal of Structural Geology 21, 7–22.

Kao, H., Angelier, J., 2001. The Chichi earthquake sequence, Taiwan: results from source parameter and stress tensor inversions. Earth and Planetary Sciences 333, 65–80.

Lee, J.C., Chu, H.T., Angelier, J., Chan, Y.C., Hu, J.C., Lu, C.Y., Rau, R.J., 2002. Geometry and structure of northern surface ruptures of the 1999 Mw = 7.6 Chi-Chi, Taiwan earthquake: influence from inherited fold belt structures. Journal of Structural Geology 24, 173–192.

Lee, Y.H., Hsieh, M.-L., Lu, S.-D., Shih, T.-S., Wu, W.-Y., Sugiyama, Y., Azuma, T., Kariyae, Y., 2003. Slip vectors of the surface rupture of the 1999 Chi-Chi earthquake, western Taiwan. Journal of Structural Geology 25, 1917–1931.

Shan, Y., Suen, H., Lin, G., 2003. Separation of polyphase fault/slip data: an objective-function algorithm based on hard division. Journal of Structural Geology 25, 829–840.

Shan, Y., Lin, G., Li, Z., 2004. A stress inversion procedure for automatic recognition of polyphase fault/slip data sets. Journal of Structural Geology 26, 919–925.

Xu, P., 2004. Determination of regional stress tensors from fault-slip data. Geophysical Journal International 157, 1316–1330.